AIP | Applied Physics Letters

Alternative p-doped hole transport material for low operating voltage and high efficiency organic light-emitting diodes

Caroline Murawski, Cornelius Fuchs, Simone Hofmann, Karl Leo, and Malte C. Gather

Citation: Applied Physics Letters **105**, 113303 (2014); doi: 10.1063/1.4896127
View online: http://dx.doi.org/10.1063/1.4896127
View Table of Contents: http://scitation.aip.org/content/aip/journal/apl/105/11?ver=pdfcov
Published by the AIP Publishing

Alternative p-doped hole transport material for low operating voltage and high efficiency organic light-emitting diodes

Caroline Murawski,[1,a)] Cornelius Fuchs,[1] Simone Hofmann,[1] Karl Leo,[1] and Malte C. Gather[1,2]
[1]*Institut für Angewandte Photophysik, Technische Universität Dresden, George-Bähr-Str. 1, 01062 Dresden, Germany*
[2]*SUPA, School of Physics & Astronomy, University of St Andrews, North Haugh, St Andrews, KY16 9SS Scotland, United Kingdom*

(Received 7 May 2014; accepted 8 September 2014; published online 18 September 2014)

We investigate the properties of N,N′-[(Diphenyl-N,N′-bis)9,9,-dimethyl-fluoren-2-yl]-benzidine (BF-DPB) as hole transport material (HTL) in organic light-emitting diodes (OLEDs) and compare BF-DPB to the commonly used HTLs N,N,N′,N′-tetrakis(4-methoxyphenyl)-benzidine (MeO-TPD), 2,2′,7,7′-tetrakis(N,N′-di-p-methylphenylamino)-9,9′-spirobifluorene (Spiro-TTB), and N,N′-di(naphtalene-1-yl)-N,N′-diphenylbenzidine (NPB). The influence of 2,2′-(perfluoronaphthalene-2,6-diylidene)dimalononitrile (F6-TCNNQ p-dopant) concentration in BF-DPB on the operation voltage and efficiency of red and green phosphorescent OLEDs is studied; best results are achieved at 4 wt. % doping. Without any light extraction structure, BF-DPB based red (green) OLEDs achieve a luminous efficacy of 35 .1 lm/W (74 .0 lm/W) at 1000 cd/m^2 and reach a very high brightness of 10 000 cd/m^2 at a very low voltage of 3.2 V (3.1 V). We attribute this exceptionally low driving voltage to the high ionization potential of BF-DPB which enables more efficient hole injection from BF-DPB to the adjacent electron blocking layer. The high efficiency and low driving voltage lead to a significantly lower luminous efficacy roll-off compared to the other compounds and render BF-DPB an excellent HTL material for highly efficient OLEDs. © *2014 AIP Publishing LLC*. [http://dx.doi.org/10.1063/1.4896127]

In order to obtain organic light-emitting diodes (OLED) with high efficiency, many studies have focused on optimizing the emission layer and very high external quantum efficiencies (EQE), close to the theoretical maximum, have indeed been achieved.[1–3] For industrial applications, however, the luminous efficacy (LE) of OLEDs is more important than the EQE as it provides a direct measure of the power consumption by taking the operating voltage into account. Typically, the efficiency of OLEDs decreases with increasing brightness (so-called efficiency roll-off). This roll-off is much more pronounced for the LE than for the EQE due to additional resistive losses.[4] In order to obtain high LE values at high brightness levels (>1000 cd/m^2), it is thus crucial to achieve high current densities at low voltage. This can be achieved by using electrically doped charge transport layers to reduce injection barriers and facilitate high conductivity.[5–7] So-called *pin*-structures, consisting of intrinsic layers sandwiched between *p*- and *n*-doped transport layers, indeed show low operating voltages close to the optical band gap of the emitter.[7,8] The *pin*-structure further allows to adjust the thickness of the *p*-doped hole transport layer (HTL) and *n*-doped electron transport layer (ETL) without affecting the electrical device properties. This facilitates an improved outcoupling efficiency by positioning the emitter at the maximum of the electromagnetic field of the microcavity mode supported by the OLED structure.[9,10] It is generally believed that the choice of the host material of the p-doped transport layer has a relatively weak influence on the efficiency of *pin*-OLEDs because the doping is expected to provide sufficient conductivity and guarantee Ohmic charge injection. Therefore, most studies have used a single host material and vary the dopant material.[11–14]

Here, we compare three widely used hole transport materials (MeO-TPD, Spiro-TTB, and NPB) with BF-DPB, a material that is less well studied in the OLED community so far but well-known in the context of organic solar cells, in particular for its good hole transport properties and high glass transition temperature.[15–17] We investigate the influence of doping concentration on the operation voltage and efficiency of red and green phosphorescent OLEDs. We find that BF-DPB and NPB based OLEDs exhibit significantly steeper *J-V* curves than devices based on the other two HTLs and thus achieve excellent luminous efficacy. BF-DPB based red-emitting OLEDs that were systematically optimized in terms of device optics and doping concentration reach a brightness of 1000 cd/m^2 at 2.6 V and achieve an LE of 35 .1 lm/W at this luminance level, without using any further outcoupling structures. These numbers are among the best reported in the literature for conventional bottom emitting designs.

The OLED fabrication was performed in a UHV-chamber (Kurt J. Lesker Co., base pressure 10^{-8} mbars). The different organic materials were evaporated onto glass substrates containing a 90 nm thick indium tin oxide (ITO) anode. Doping concentration, HTL material, and layer thickness are varied using shadow masks and gradient shutters, which allows fabrication of several samples within one run and thus ensures good comparability. The layer thickness is monitored *in-situ* using quartz crystal monitors. After fabrication, all OLEDs are encapsulated under nitrogen

[a)]Author to whom correspondence should be addressed. Electronic mail: caroline.murawski@iapp.de

atmosphere using glass lids and epoxy resin. All materials were purchased from commercial suppliers and purified further by vacuum gradient sublimation prior to use. Current density-voltage-luminance characteristics and spectral radiance of all OLEDs are measured with an automated system containing a source-measure unit (Keithley SM2400), a calibrated spectrometer (Instrument Systems GmbH CAS140CT), and a silicon photodiode. The EQE and LE are calculated from data measured in an Ulbricht sphere (Labsphere LMS-100), which is coupled to a calibrated spectrometer (Labsphere CDS-600). Here, the substrate edges were covered to eliminate edge emission. For absorbance measurements, single layers of the organic material were deposited on glass substrates and characterized with a spectral photometer (Shimadzu UV-3101). The conductivity of doped HTLs is measured during evaporation by depositing the respective material onto a substrate containing two parallel stripes of ITO and monitoring the current between the stripes at a pre-determined voltage.

The organic materials used in this study are N,N,N′,N′-tetrakis(4-methoxyphenyl)-benzidine (MeO-TPD), 2,2′,7,7′-tetrakis(N,N′-di-p-methylphenylamino)–9,9′-spirobifluorene (Spiro-TTB), N,N′-di(naphtalene-1-yl)-N,N′-diphenylbenzidine (NPB), and N,N′-[(Diphenyl-N,N′-bis)9,9,-dimethyl-fluorene-2-yl]-benzidine (BF-DPB) each doped with the p-dopant 2,2′-(perfluoronaphthalene-2,6-diylidene)dimalononitrile (F_6-TCNNQ) as HTL, NPB as electron blocking layer (EBL), bis-(2-methyl-8-chinolinolato)–(4-phenyl-phenolato)-aluminium(III) ($BAlq_2$) or 4,7-diphenyl-1,10-phenanthroline (BPhen) as hole blocking layer (HBL), and Cs-doped BPhen as ETL. We fabricated red and green phosphorescent OLEDs using the emitters iridium(III)bis(2-methyldibenzo[f,h]quinoxaline) (acetylacetonate) ($Ir(MDQ)_2$(acac)) and bis(2-phenylpyridine) iridium acetylacetonate ($Ir(ppy)_2$(acac)), respectively. The emission layer (EML) is formed by 20 nm NPB:$Ir(MDQ)_2$(acac) (10 wt. %) or a double-layer of 8 nm TCTA:$Ir(ppy)_2$(acac) and 12 nm TPBi:$Ir(ppy)_2$(acac) (each with 8 wt. % emitter concentration). Finally, 100 nm of either Ag or Al are used as cathode.

Fig. 1(a) shows the chemical structures of the four HTL materials, and Table I summarizes several material parameters. MeO-TPD and NPB have very low glass transition temperatures (67 and 95 °C, respectively), which is known to lead to undesired crystallization of the material in thin films.[18] Spiro-TTB and BF-DPB instead provide higher stability with glass transition temperatures of 146 and 160 °C, respectively. Compared to MeO-TPD and Spiro-TTB, BF-DPB and NPB have higher ionization potentials (IP) (5.23 and 5.4 eV) and BF-DPB and Spiro-TTB provide the highest hole mobility (5.7×10^{-5} $cm^2/(V\ s)$). However, at the same doping concentration (4 wt. % F_6-TCNNQ), the conductivity of p-BF-DPB is one order of magnitude lower than the conductivity of p-MeO-TPD and p-Spiro-TTB, presumably because the higher IP of BF-DPB renders doping with F_6-TCNNQ less efficient.

Fig. 1(b) shows the absorption spectra for all HTL materials investigated in this study. The main absorption occurs in the UV-region between 300 and 400 nm, whereas the materials are mostly transparent in the visible wavelength regime. BF-DPB and NPB, however, show a slightly higher

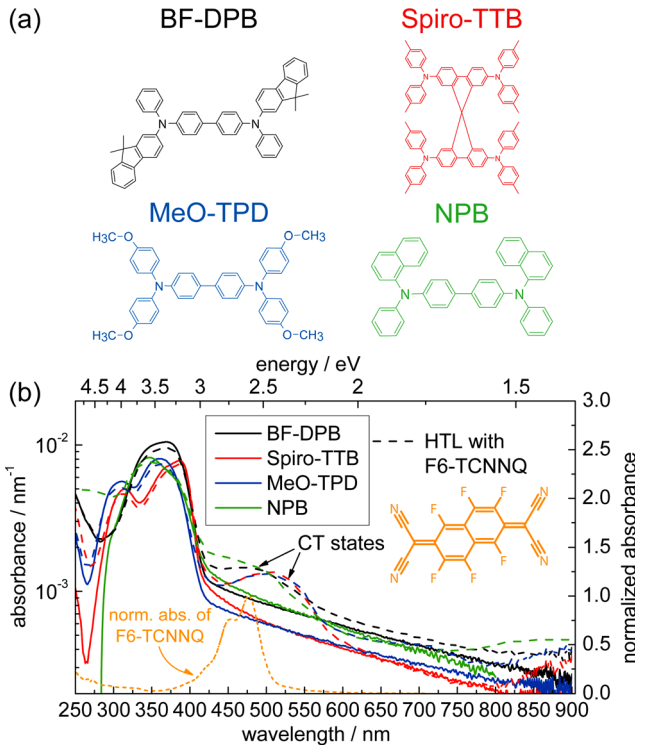

FIG. 1. (a) Molecular structures of the different HTL materials investigated in this study. (b) Thickness normalized absorbance for neat (solid line) and F_6-TCNNQ-doped (4 wt. %, dashed line) HTL layers (ca. 60 nm film on glass substrate). The dotted line shows the normalized absorption of F6-TCNNQ on linear scale. Data of F6-TCNNQ and NPB:F6-TCNNQ (3%) are taken from Ref. 19. The inset shows the molecular structure of the p-dopant F_6-TCNNQ.

residual absorption above 400 nm than the other two materials. The absorbance spectrum of F_6-TCNNQ (also known as F_6-TNAP[19]) in solution shows a maximum at 480 nm. When doping the HTLs with 4 wt. % F_6-TCNNQ, an increased absorption between 450 and 570 nm is observed for all four materials, which is attributed to the π–π*-transition of the cations/charge transfer (CT) states within the HTL and provides direct evidence for successful doping.[11,19,20] However, the absorption of F_6-TCNNQ may also contribute to the absorbance in this spectral region. Another absorption band of the p-doped HTLs is observed in the infrared region, above 850 nm, and can be ascribed to the F_6-TCNNQ anion.[19]

Menke *et al.* showed that for BF-DPB doping concentrations of around 10 wt. % F_6-TCNNQ are required to reach the same conductivity as achieved in MeO-TPD doped with F_6-TCNNQ at 4 wt. %.[13] However, besides the conductivity of the HTL its optical properties are also important for the performance of OLEDs as excessive absorption of the CT state could reduce efficiency. Therefore, we further investigate the influence of the doping concentration of BF-DPB:F_6-TCNNQ in red and green OLEDs. The OLED structure is as follows: 90 nm ITO|60 nm BF-DPB:F_6-TCNNQ (1–12 wt. %)|10 nm NPB|20 nm EML|10 nm $BAlq_2$|50 nm (green OLEDs) or 65 nm (red OLEDs) BPhen:Cs|100 nm aluminum.

Fig. 2(a) shows the current density versus the F_6-TCNNQ doping concentration of the red and green OLEDs at 3.0 V and 3.5 V, respectively. The current density first increases with increasing doping concentration. At around 4 wt. %, the current density in the green OLEDs saturates

TABLE I. Basic properties of the HTL materials BF-DPB, Spiro-TTB, MeO-TPD, and NPB including glass-transition temperature, ionization potential, hole mobility, and conductivity. Conductivity was measured for an HTL doped with 4 wt. % F_6-TCNNQ.

	BF-DPB	Spiro-TTB	MeO-TPD	NPB
Glass-transition temperature (°C)	160[15]	146[18]	67[27]	95[28]
IP[a] (eV)	5.23[15]	5.1[29]	5.07[14]	5.4[30]
Mobility[b] (cm^2/(V s))	5.7×10^{-5} (Ref. 13)	5.7×10^{-5} (Ref. 18)	2.3×10^{-5} (Ref. 13)	2.4×10^{-5} (Ref. 31)
Conductivity (S/cm)	1.8×10^{-5}	1.3×10^{-4}	1.5×10^{-4}	N/A[c]

[a]Measured by ultraviolet photoelectron spectroscopy.
[b]Extracted from FET measurements.
[c]Not measured.

and for the red OLEDs the slope is strongly reduced, i.e., the increase in current density with a further increase in doping is much lower. Therefore, for applications of BF-DPB in OLEDs, a doping concentration of 4 wt. % F_6-TCNNQ appears to be sufficient. This is in agreement with earlier findings for F_6-TCNNQ doping of MeO-TPD and Spiro-TTB.[13,21]

Fig. 2(b) summarizes the external quantum efficiency of the investigated OLEDs at 15.4 mA/cm^2. For the red-emitting OLEDs, the EQE remains constant for all doping concentrations (within the measurement error). For the green-emitting devices, however, the EQE steadily decreases from 15.5% at 1 wt. % doping to 13.1% at 12 wt. %. The decrease in EQE for the green-emitting devices is attributed to the increased absorption by CT states, which absorb in the blue and green wavelength regimes but not in the red (cf. Fig. 1(b)). As an optimal trade-off between conductivity and absorption loss, we choose a doping concentration of 4 wt. % for all following experiments.

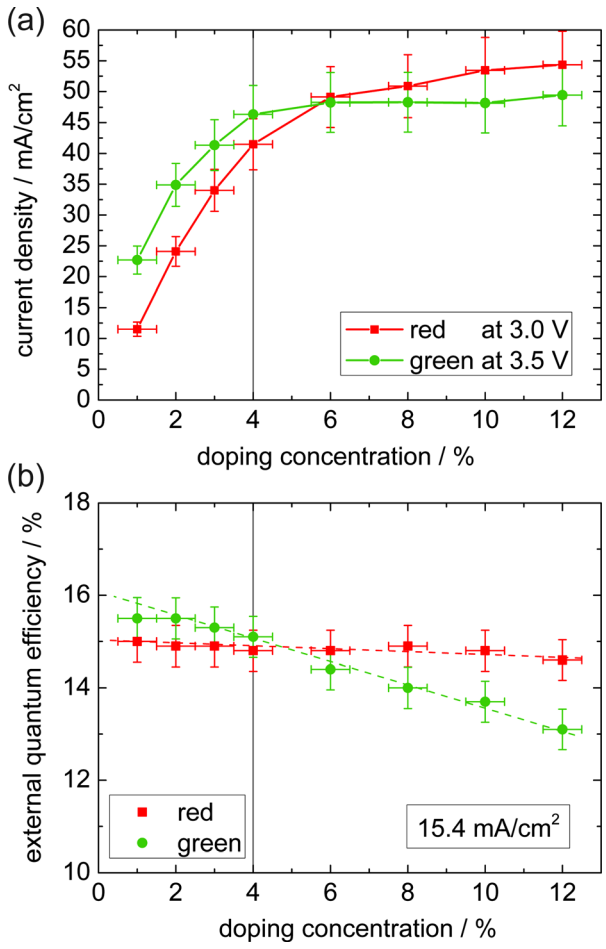

FIG. 2. Influence of p-doping concentration (dopant: F_6-TCNNQ) in the BF-DPB HTL of red- and green-emitting phosphorescent *pin*-OLEDs. (a) Current density as a function of the doping concentration, measured at 3 V (3.5 V) for red (green) devices. Lines are guides to the eye. (b) External quantum efficiency of same devices, measured at 15.4 mA/cm^2. Dashed lines are linear fits.

In a next step, we compare the performance of the four HTL materials in red and green OLEDs. Figs. 3(a) and 3(d) show the OLED structure used. In contrast to the preceding series of devices discussed, the device structures are now fully optimized in terms of transport layer thicknesses and HBL and cathode material in order to achieve highest possible luminous efficacy. The emission spectrum is not influenced by the choice of HTL; the electroluminescence spectra are identical for all four HTLs (cf. insets in Figs. 3(c) and 3(f)).

The choice of HTL material strongly influences the current-voltage characteristics, especially for the red OLEDs (cf. Figs. 3(b) and 3(e)). For any given voltage, the highest current density is achieved when using BF-DPB, followed by NPB, Spiro-TTB, and MeO-TPD. This indicates that the current density in these devices is limited by the p-side. We attribute the stronger effect for red OLEDs to the fact that the energy barrier for hole injection from the EBL to the emitter is negligible for the red structures (0.05 eV) thus allowing efficient hole injection. Within the operating voltage range of our devices (2.5–5 V), BF-DPB and NPB based OLEDs show a five-fold higher current density than the MeO-TPD based device. We attribute this significant improvement in current density to the higher IPs of BF-DPB and NPB (Table I), which reduce the energy barrier for hole injection from the HTL to the undoped EBL. The injection of holes from the ITO anode into the HTL is not disturbed by the high IP of the HTL as the p-doping leads to effective band-bending at this interface. The onset of light output (2.3 V for red and 2.6 V for green OLEDs) is close to the intrinsic limit of the emitter and similar for all four HTL materials. Furthermore, the luminance increases very quickly, reaching 10 000 cd/m^2 at 3.2 V for red and 3.1 V for green OLEDs using BF-DPB as HTL.

The external quantum efficiency and luminous efficacy of all devices are shown in Figs. 3(c) and 3(f). Table II summarizes the performance at 1000 cd/m^2. For the red OLEDs, the highest EQE (20.0%) is obtained with MeO-TPD as HTL. Using BF-DPB leads to a slightly lower EQE (18.9% at 1000 cd/m^2). However, due to its favorable *J-V* characteristics, the BF-DPB based OLED achieves the highest LE

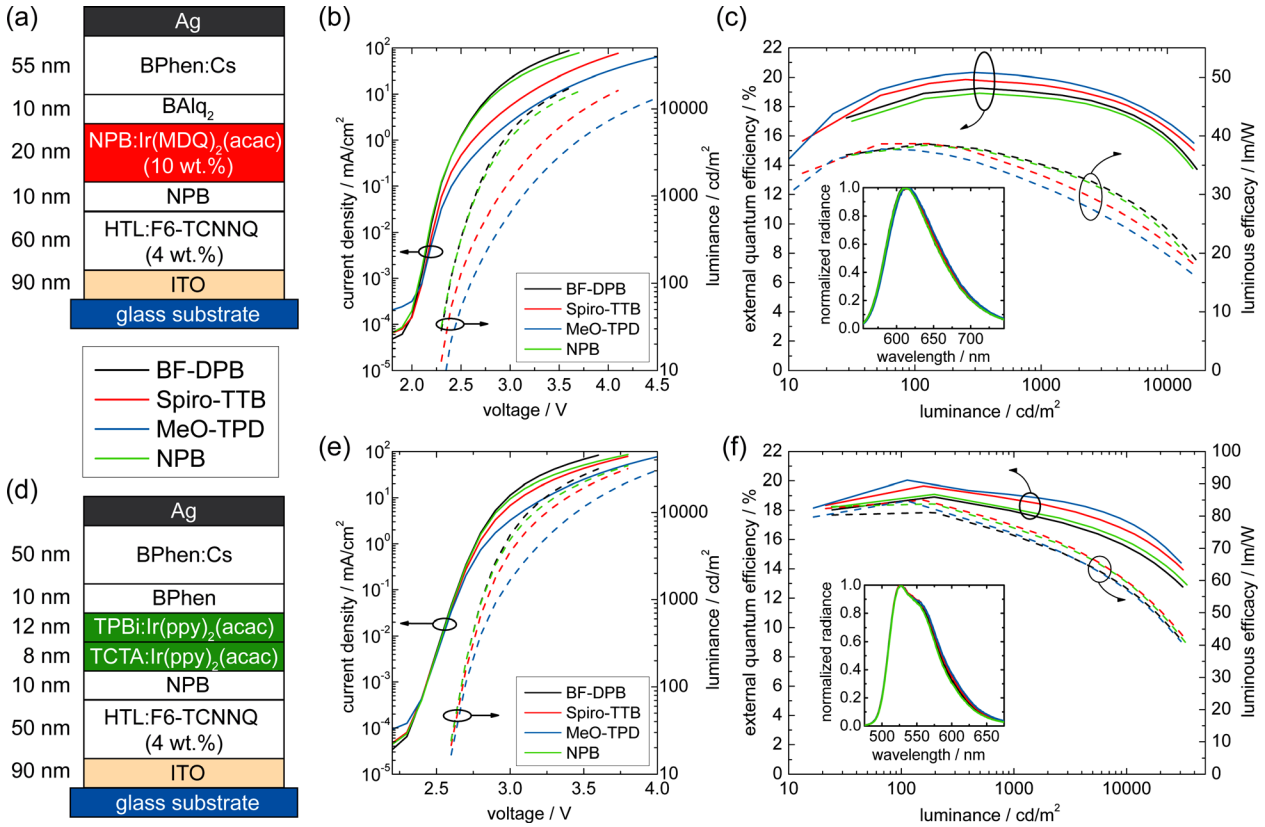

FIG. 3. Performance of optimized red- ((a)–(c)) and green-emitting ((d)–(f)) OLEDs with different HTL materials. (a) and (d) OLED layer structure. (b) and (e) Current density (solid lines) and luminance (dashed lines) *vs.* voltage. (c) and (f) External quantum efficiency (solid lines) and luminous efficacy (dashed lines) as a function of luminance. The inset shows the normalized EL spectra at 1000 cd/m^2.

among the tested devices (35.1 lm/W at 1000 cd/m^2). To the best of our knowledge, this value is the highest reported luminous efficacy value for red bottom-emitting OLEDs without additional outcoupling structures.[22–24] Higher LEs were only achieved in top-emitting devices or more specialized structures exhibiting higher microcavity quality factors.[25,26] However, strong microcavities usually suffer from strong angle-dependent emission color shifts, which make them unsuitable for lighting applications. Optical simulations indicate that if all light that is trapped in the substrate could be extracted, e.g., by using a macroscopic outcoupling lens, the LE of our devices would further improve to 66.6 lm/W at 1000 cd/m^2.

For the green OLEDs, the trend in EQE for the different HTL materials is similar to the behavior of the red OLEDs (cf. Fig. 3(f)): BF-DPB and NPB have a slightly reduced EQE compared to MeO-TPD and Spiro-TTB. The luminous efficacy is nearly the same for all HTL materials, ranging from 74 to 77 lm/W at 1000 cd/m^2 (again without outcoupling structures). Here, our simulations indicate that the LE for BF-DPB based OLEDs could be further improved to 147.9 lm/W if all light from glass modes could be extracted.

It is worth noting that the steep *J*-*V*-curves using BF-DPB are especially favorable for lighting application of OLEDs where the devices are driven at brightness levels up to 5000 cd/m^2 and where the higher resistance of the other HTL materials will lead to stronger roll-off in LE.

In conclusion, we compared BF-DPB, a high glass transition temperature material that was not used as HTL in OLEDs so far, to the commonly used HTL materials MeO-TPD, Spiro-TTB, and NPB. Absorption measurements show that doping of the HTL materials with the p-dopant F_6-TCNNQ leads to the formation of CT states with absorption in the blue part of the visible spectrum. For OLEDs with F_6-TCNNQ doped BF-DPB, the optimal tradeoff between high current densities and good EQE is reached at 4 wt. % F_6-TCNNQ doping. We then compared the four HTL materials in optically optimized red and green OLEDs. BF-DPB provides the best current-voltage characteristics of all four materials due to its high IP, which favors hole injection into the adjacent EBL. Red and green OLEDs reached a very high luminance of 10 000 cd/m^2 already at 3.2 V and 3.1 V and achieved LEs of 35.1 lm/W and 74.0 lm/W at 1000 cd/m^2, respectively, without any light extraction structure. These values are among the highest reported so far.

TABLE II. Performance of red and green OLEDs at 1000 cd/m^2 comprising the four different HTL materials tested here.

	HTL	EQE (%)	LE (lm/W)	CE (cd/A)	Voltage (V)
Red	BF-DPB	18.9	35.1	27.1	2.6
	Spiro-TTB	19.5	33.3	27.7	2.9
	MeO-TPD	20.0	31.4	26.2	3.1
	NPB	18.6	34.9	27.7	2.7
Green	BF-DPB	17.9	74.0	53.4	2.8
	Spiro-TTB	19.7	77.0	54.4	2.8
	MeO-TPD	19.0	74.6	52.4	2.9
	NPB	18.1	76.3	56.2	2.8

BF-DPB offers good thermal stability and a low LE roll-off, which makes it a suitable candidate for high brightness applications. Overall, our investigations show that BF-DPB is a valid alternative to the widely used MeO-TPD, Spiro-TTB, and NPB as HTL material in OLEDs.

We thank Markus Fröbel and Torben Menke for conductivity measurements. This work received funding from the European Community Seventh Framework Programme under Grant Agreement No. FP7 267995 (NUDEV) and from the European Social Fund and the free state of Saxony through the OrganoMechanics project.

[1]L. Xiao, Z. Chen, B. Qu, J. Luo, S. Kong, Q. Gong, and J. Kido, Adv. Mater. **23**, 926 (2011).
[2]Z. B. Wang, M. G. Helander, J. Qiu, D. P. Puzzo, M. T. Greiner, Z. W. Liu, and Z. H. Lu, Appl. Phys. Lett. **98**, 073310 (2011).
[3]S. Reineke, F. Lindner, G. Schwartz, N. Seidler, K. Walzer, B. Lüssem, and K. Leo, Nature **459**, 234 (2009).
[4]C. Murawski, K. Leo, and M. C. Gather, Adv. Mater. **25**, 6801 (2013).
[5]M. Pfeiffer, T. Fritz, J. Blochwitz, A. Nollau, B. Plönnigs, A. Beyer, and K. Leo, Adv. Solid State Phys. **39**, 77 (1999).
[6]B. Lüssem, M. Riede, and K. Leo, Phys. Status Solidi A **210**, 9 (2012).
[7]T. Matsushima and C. Adachi, Appl. Phys. Lett. **89**, 253506 (2006).
[8]J. Huang, M. Pfeiffer, A. Werner, J. Blochwitz, K. Leo, and S. Liu, Appl. Phys. Lett. **80**, 139 (2002).
[9]K. Walzer, B. Maennig, M. Pfeiffer, and K. Leo, Chem. Rev. **107**, 1233 (2007).
[10]M. Furno, R. Meerheim, S. Hofmann, B. Lüssem, and K. Leo, Phys. Rev. B **85**, 115205 (2012).
[11]C.-H. Gao, X.-Z. Zhu, L. Zhang, D.-Y. Zhou, Z.-K. Wang, and L.-S. Liao, Appl. Phys. Lett. **102**, 153301 (2013).
[12]J.-H. Lee, D.-S. Leem, H.-J. Kim, and J.-J. Kim, Appl. Phys. Lett. **94**, 123306 (2009).
[13]T. Menke, D. Ray, H. Kleemann, M. P. Hein, K. Leo, and M. Riede, Org. Electron. **15**, 365 (2014).
[14]M. L. Tietze, L. Burtone, M. Riede, B. Lüssem, and K. Leo, Phys. Rev. B **86**, 035320 (2012).
[15]R. Meerheim, S. Olthof, M. Hermenau, S. Scholz, A. Petrich, N. Tessler, O. Solomeshch, B. Lüssem, M. Riede, and K. Leo, J. Appl. Phys. **109**, 103102 (2011).
[16]Y. H. Kim, C. Sachse, M. Hermenau, K. Fehse, M. Riede, L. Müller-Meskamp, and K. Leo, Appl. Phys. Lett. **99**, 113305 (2011).
[17]M. Hermenau, S. Schubert, H. Klumbies, J. Fahlteich, L. Müller-Meskamp, K. Leo, and M. Riede, Sol. Energy Mater. Sol. Cells **97**, 102 (2012).
[18]T. P. I. Saragi, T. Fuhrmann-Lieker, and J. Salbeck, Adv. Funct. Mater. **16**, 966 (2006).
[19]P. K. Koech, A. B. Padmaperuma, L. Wang, J. S. Swensen, E. Polikarpov, J. T. Darsell, J. E. Rainbolt, and D. J. Gaspar, Chem. Mater. **22**, 3926 (2010).
[20]X. Zhou, J. Blochwitz, M. Pfeiffer, A. Nollau, T. Fritz, and K. Leo, Adv. Funct. Mater. **11**, 310 (2001).
[21]C. Murawski, P. Liehm, K. Leo, and M. C. Gather, Adv. Funct. Mater. **24**, 1117 (2014).
[22]D. H. Kim, N. S. Cho, H.-Y. Oh, J. H. Yang, W. S. Jeon, J. S. Park, M. C. Suh, and J. H. Kwon, Adv. Mater. **23**, 2721 (2011).
[23]C.-H. Chien, F.-M. Hsu, C.-F. Shu, and Y. Chi, Org. Electron. **10**, 871 (2009).
[24]Y. Zhao, J. Chen, and D. Ma, ACS Appl. Mater. Interfaces **5**, 965 (2013).
[25]R. Meerheim, R. Nitsche, and K. Leo, Appl. Phys. Lett. **93**, 043310 (2008).
[26]S. Hofmann, M. Thomschke, P. Freitag, M. Furno, B. Lüssem, and K. Leo, Appl. Phys. Lett. **97**, 253308 (2010).
[27]M. Thelakkat, R. Fink, F. Haubner, and H.-W. Schmidt, Macromol. Symp. **125**, 157 (1997).
[28]S. A. Van Slyke, C. H. Chen, and C. W. Tang, Appl. Phys. Lett. **69**, 2160 (1996).
[29]M. Schober, M. Anderson, M. Thomschke, J. Widmer, M. Furno, R. Scholz, B. Lüssem, and K. Leo, Phys. Rev. B **84**, 165326 (2011).
[30]M. Schober, S. Olthof, M. Furno, B. Lüssem, and K. Leo, Appl. Phys. Lett. **97**, 013303 (2010).
[31]C. H. Cheung, K. K. Tsung, K. C. Kwok, and S. K. So, Appl. Phys. Lett. **93**, 083307 (2008).